Sasaki *et al. Robomech J (2015) 2:13*
DOI 10.1186/s40648-015-0037-8

ROBOMECH Journal
a SpringerOpen Journal

RESEARCH ARTICLE

Open Access

Shoulder joint contact force during lever-propelled wheelchair propulsion

Makoto Sasaki[1*], Dimitar Stefanov[2], Yuki Ota[1], Hiroki Miura[3] and Atsushi Nakayama[3]

Abstract

The aim of this study was to obtain quantitative results about shoulder contact force during wheelchair lever propulsion when the gear ratio of the lever propulsion mechanism is changing. The effect of the gear ratio on the shoulder contact force was investigated for few different wheelchair loading. For the experiments we designed a special mechatronic wheelchair simulator that allowed the simulation of different gear ratios of the wheelchair lever propulsion mechanism and simulation of different road inclinations. The same simulator was also used for simulation of a hand rim propelled wheelchair. We conducted also a handrim propulsion experiment and used the results from it for comparison with the lever propulsion data. Four nondisabled male adults with no prior wheeling experience participated in the experiment. In the first tests, a lever propelled wheelchair was simulated with the simulator. The target speed of the wheelchair was set to 2 km/h. For the test, the gear ratio was varied from 1.5 to 1/1.5. A load torque was applied to the rear wheels to imitate road inclinations of 0°, 2° and 4°. In the second part of the test, the simulator was structured to simulate a handrim propelled wheelchair. The participants were asked to keep the same speed (2 km/h) and the simulator was set sequentially to imitate climbing a ramp inclined on 0°, 2° and 4°. Kinematic data of the body were collected by a motion capture system. Kinetic data such as hand force and driving torque, were measured by instrumented wheels with incorporated six-axis force sensor. The intersegmental joint forces and moments were calculated from the obtained kinematic and kinetic data via inverse dynamics analysis procedure. Muscle forces were computed from the measured joint moments by using an optimization approach. Shoulder joint contact force, which indicates the joint surface loading, was computed as a synthetic vector of the intersegmental force for shoulder joint acquired from the inverse dynamics analysis and the compressive forces from muscles, tendons, ligaments and cartilages crossing the shoulder joint. It was observed that the decrease of the gear ratio causes increased cycle frequency and reduces the shoulder joint contact force. Result showed that the shoulder joint contact force during lever propulsion with a gear ratio 1/1.5 was up to 70 % lower than the shoulder joint contact force during handrim propulsion. The results from this study could be used in the design of new lever propulsion mechanisms that reduce the risks of secondary shoulder disorders and increase user's comfort.

Keywords: Lever-propelled wheelchair, Musculoskeltal model, Shoulder joint contact force

Background

Wheelchair handrim propulsion comprises a push phase in which the user applies force to the handrims to generate propulsion torque around the wheel axle, and a recovery phase when the user releases the hands from the handrims to initiate the next push phase. However, the mechanical efficiency of the wheelchair propulsion is quite low, usually about 10 % [1–3]. The propulsion torque transmitted to the driving wheel depends on the tangential component of the force applied to the handrim by user's hand, handrim radius, and the torque around the point of hand contact. In general, the hand force in tangential direction toward the handrim contributes to the wheelchair propulsion because the handrim has only one degree of freedom which is its rotation around the rear wheel axis [4]. However, wheelchair user needs to impose a significant force in normal direction toward the handrim in order to create a frictional force and achieve

*Correspondence: makotosa@iwate-u.ac.jp
[1] Graduate School of Engineering, Iwate University, Morioka, Iwate, Japan
Full list of author information is available at the end of the article

efficient wheelchair propulsion. Usually, a significant part of the energy for wheelchair propulsion is used for generation of the normal force. The normal force does not contribute to the torque transferred to the driving wheel and decreases the energy efficiency. Propulsion efficiency also depends on the manner of application of propulsion force used by the individual and it is reduced additionally due to the intermittent character of the force applied to the handrims. Groot et al. investigated the effect of the visual feedback on the generated handrim wheelchair force and gross mechanical efficiency [5]. It was found that visual feedback could be a useful learning tool that helps for improvement of the effective force direction and higher effective force production but it was also noticed that the control group that did not use visual feedback showed a better gross mechanical efficiency compared to the experimental group. A quantitative analysis of the wheelchair manoeuvrability from a viewpoint of upper limb manipulability has been presented in [6]. The same study compared the effective force direction with the direction of the maximum force estimated from the measured maximum joint torques of an upper limb model with 7 d.o.f. It was found that maximum propulsion efficiency is achieved when the direction of the applied force is closer to tangent to the handrim in the contact point. Analysis showed that the direction of the estimated maximum force changes significantly during the push phase. Especially, at the beginning of the push phase the direction of the estimated maximum force is quite different from tangential direction. That decreases propulsion efficiency and increases physical load to the user.

An average wheelchair user usually performs about 2000–3000 propulsion motions a day. Reportedly, as a result of the wheelchair propulsion, more than half of the long-term wheelchair users experience secondary disorders such as arthralgia, rotator cuff tear, ulnar nerve injury, and carpal tunnel syndrome [7–10]. The problem inspired many research studies essentially linked with the improvement of the mechanical efficiency of the wheelchair propulsion and reducing physical load [11–15].

Lever-propulsion mechanisms became a strong alternative to the handrim propulsion. Numerous design solutions employ a lever which length is longer than the handrim radius. It has been demonstrated that the lever-propulsion mechanisms possess few significant advantages to the handrim propulsion. Brubaker et al. established that mechanical efficiency of the lever propulsion is higher than that of handrim propulsion [1]. The same authors also suggested that lever propulsion could be applicable to a wide range of individuals because the mechanical efficiency remains slightly affected by the changes of the seat positions. Hughes et al. compared the patterns of changing the shoulder and elbow joint angles during lever propulsion and handrim propulsion at various seat positions and demonstrated that joint angles during handrim propulsion experiment change in much bigger range [11]. This result was supported by the findings of Brubaker et al. [1]. Requejo et al. examined the EMG (electromyography) signal around shoulder joint area and revealed that the muscle activities of the supraspinatus and the sternal and clavicular portion of the pectoralis major during lever propulsion are significantly lower, which indicated that physical load during lever propulsion is significantly reduced [15]. These results suggested that lever propulsion may mitigate the risk of secondary joint disorders. Jordon Lui et al. compared the energy efficiency of two commercially available lever propulsion wheelchair mechanisms with those of a handrim mechanism. Results reveal that the oxygen uptake (VO_2) and heartrate of the subjects participating in the experiments were significantly lower during the lever propulsion tests, which indicated that the mechanical efficiency of lever propulsion mechanisms could be significantly higher compared to the handrim propulsion [16].

Handrim propulsion causes detrimental compressive joint contact forces that could contribute to the development of a shoulder impingement syndrome. Because of that the importance of the problem, the mechanisms of the development of these forces and approaches for their reduction have been a topic of many research studies [17–19]. Vegger et al. examined shoulder joint contact force for two wheelchair speeds and two levels of resistance by using kinematic data and kinetic data from a sensored handrim. Their study revealed that shoulder contact force is relatively low when wheelchair propulsion has low-intensity [18]. Morrow et al. used kinematic and kinetic data to estimate shoulder joint contact force during various arm loadings such as level propulsion, ramp propulsion, and weight relief lift activities. They revealed that shoulder joint contact forces during ramp propulsion and weight relief lift activities are markedly higher than those during level propulsion [19].

Studies on the shoulder joint contact forces give important knowledge on prevention of secondary disorders, such as pain in the arm and new wheelchair design. However, there is no quantitative information about shoulder joint contact force during lever propulsion.

In this study we conducted series of experiments to examine the effect of gear ratio of the lever propulsion mechanism on the shoulder joint contact force quantitatively. For the experiments, we developed a special mechatronic wheelchair simulator that allows simulation of lever propulsion on various gear ratios and road inclinations.

Lever propulsion mechanisms possess few adjustable parameters. That offers more options for individual adjustment of the lever-propelled wheelchair to the movement abilities of the particular user. However, in certain patient cases it is difficult for the assessor to find the best configuration (lever length and gear ratio) that will cause minimal shoulder joint contact force while keeping the propulsion optimal. Present study investigates shoulder joint contact forces for few different gear ratios. The results could inform prescription and adjustment of wheelchair lever propulsion mechanisms, making them easier and much precise.

Methods

Subjects

Four nondisabled male adults with no prior wheeling experience (age, 22.2 ± 0.4 years mean ± SD; height, 172.0 ± 6.7 cm; weight, 59.6 ± 5.0 kg; forearm length, 24.6 ± 1.7 cm) participated in the experiment. The tests were conducted after their approval by the Ethical Review Board of Iwate University. Before the start of the trials, the study objective, experimental protocol and risks were explained to each subject and a written consent was taken.

Wheelchair simulator

A wheelchair simulator of wheelchair handrim propulsion was developed by the authors for their previous research [13]. It allowed simulation of wheelchairs with different geometry by changing the horizontal position of the seat and its height, distance between driving wheels, seat angle, and backrest angle. The distance between the seat section and the rear wheels was set by six linear actuators controlled by a PC. Various road resistances were simulated by a powder brake connected to the rear wheels through a roller and a timing belt. For the new tests, the existed simulator was upgraded to allow simulation of lever propulsion on various gear ratios and road inclinations. In this study, the powder brake was replaced with an AC servo motor (SGMCS-35E3B41; Yaskawa Electric Co., Japan) controlled by a PC (Fig. 1). The kinetic data were measured by a six-axis force sensor, as shown in Fig. 1.

The block diagram of the developed servo motor control system is shown in Fig. 2, where $\dot{v}_{ref}$ denotes wheelchair's target speed and τ_r, τ_l represent the input torque imposed by the subject to the right and left wheel.

The gear ratio of the lever propulsion mechanism is determined as following (Fig. 3):

$$Gear\ ratio\ G_R = wheel\ angle\ \theta_w / lever\ angle\ \theta_h \quad (1)$$

The disturbance torque is given as follows:

$$\tau_d = RMg \sin\alpha \quad (2)$$

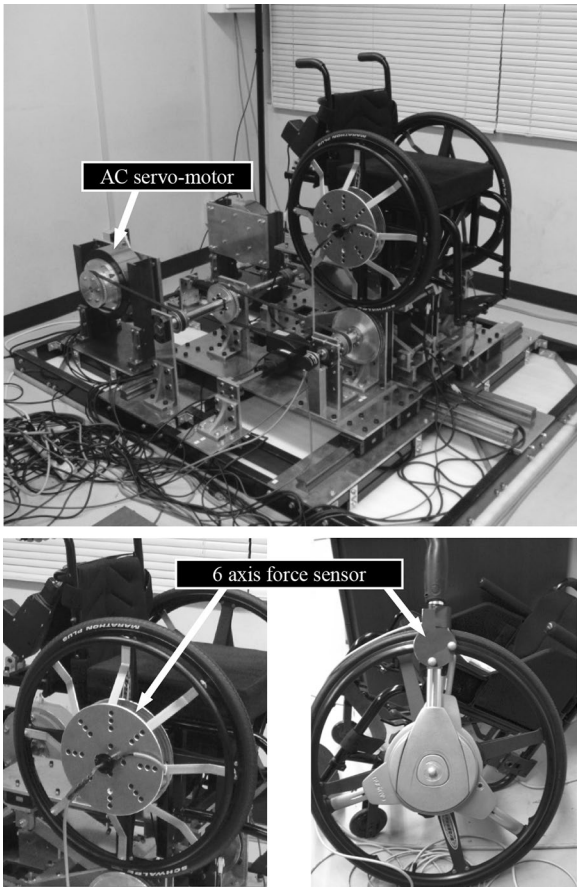

Fig. 1 Wheelchair simulator

where, R is radius of rear wheel, M is mass of subject and wheelchair, g is acceleration of gravity, and α is inclination angle. The resultant wheelchair speed is given by

$$\dot{v} = \frac{R}{Js + D}\left(\frac{\tau_r + \tau_l}{G_R} - \tau_d\right) \quad (3)$$

where, J is moment of inertia and D is frictional resistance of wheelchair.

Instrumentation and data collection

A motion capture system (OptiTrack; NaturalPoint, Inc.) was used for three-dimensional measurements of user's body (kinematic data) (Fig. 4). The motion capture system contained 12 infrared cameras (FLEX: V100R2) positioned around the wheelchair simulator. Reflective markers were attached on 34 anatomical landmarks on the whole body on the subjects.

For the handrim propulsion experiment, kinetic data were acquired by an instrumented wheel comprising a handrim connected to a wheelchair wheel [model HHR-4; OX Engineering Co. Ltd., Japan, diameter 595 mm (24 inches)] via a six-axis force sensor (model

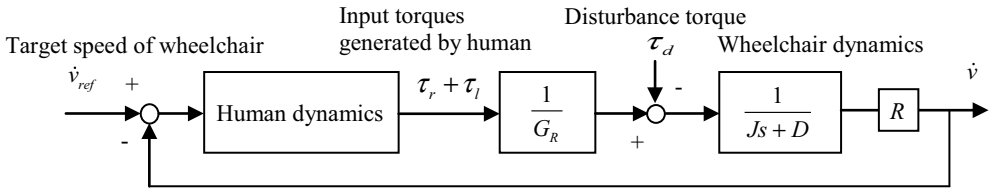

Fig. 2 Block diagram of control system for a wheelchair simulator

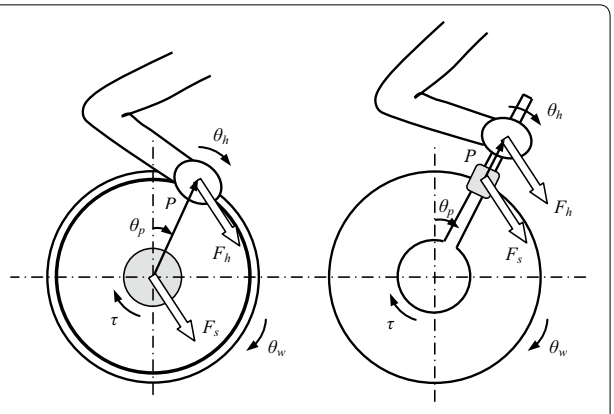

a Handrim type **b** Lever type

Fig. 3 Definition of model parameters

Fig. 4 Overview of the motion capture system and the landmarks

IFS-45E15A250-I63-ANA; Nitta Corp.) (Fig. 1). The handrim had a radius of 266.7 mm. The seat position was aligned vertically to the wheel axle. For that purpose, the subject was asked to hold his arm in vertical position and the seat was moved in a horizontal direction until the middle finger was positioned in line with the rear wheel axis. Then, the seat was elevated or lowered until the tip of the middle finger met the rear wheel axis.

For the lever propulsion experiment we utilized a commercially available lever-propulsion mechanism (NuDrive; Pure Global Ltd., UK) connected to a wheelchair wheel with a diameter 595 mm, model HHR-4; OX Engineering Co. Ltd., Japan,. A six-axis force sensor (IFS-67M25T50-M40BS-ANA; Nitta Corp.) was incorporated at the grip root of the lever-propulsion mechanism for collecting kinetic data (Fig. 1). The seat position was adjusted on the same way as in the handrim propulsion experiment. The subject was asked to grasp the grip of the lever by keeping his middle finger on a marking tape glued on 420 mm from the lever fulcrum.

The subjects were instructed to keep target speed of 2 km/h during the experiments. For providing visual feedback to the subject, the wheelchair speed was displayed on a computer screen mounted in front of the user. The disturbance torque was applied to the rear wheels. For these experiments, the disturbance torque was set to simulate road inclinations of 0°, 2° and 4°. The wheelchair seat was set horizontal. For the lever propulsion tests we used three gear ratios: 1.5, 1, and 1/1.5.

Each propulsion test continued 3 min and was performed twice. The sampling frequency of the kinematic and kinetic data was 100 Hz.

Musculoskeletal model

nMotion musculous musculoskeletal model (nac Image Technology Inc.) based on the study of Nakamura et al. [20, 21], was used for analysis of the wheelchair propulsion (Fig. 5). nMotion musculous is widely used for analysis of various movements, including studies on baseball pitching and sprint running [22–25]. The musculoskeletal model used in this study comprised 997 muscles, 50 tendons, 125 ligaments, 34 cartilages, 53 group of bones, and 155 degrees of freedom of joints, including 47 muscles participating in motion of the shoulder joint and 3 degrees of freedom of the shoulder joint (flexion/extension, adduction/abduction, and external rotation/internal rotation).

Kinematic data, marker position data obtained by an optical motion capture system, were used for computation of the angles $\boldsymbol{q}$, angular velocities $\dot{\boldsymbol{q}}$ and angular

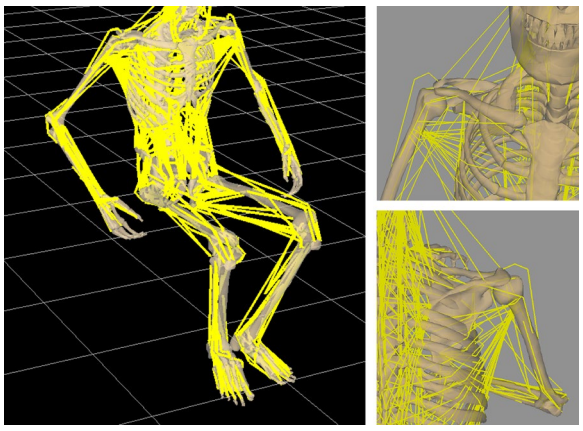

Fig. 5 Musculoskeletal model used for wheelchair propulsion analysis

accelerations $\ddot{\boldsymbol{q}}$ of each joint. The following procedure was followed for optimization of the computation process:

Find $\boldsymbol{q}$ that minimizes

$$Z = \frac{1}{2}\sum_{i=1}^{N_M} \left|\hat{\boldsymbol{p}}_i - \boldsymbol{p}_i(\boldsymbol{q})\right|^2 \tag{4}$$

subject to

$$l_j(\boldsymbol{q}) < \hat{l}_j \quad (0 < j < N_T) \tag{5}$$

where, $\boldsymbol{q} \in \mathrm{R}^{N_J}$ are joint angles, N_J is the total number of degree of freedom for all joints, N_M is the total number of markers, $\hat{\boldsymbol{p}}_i \in \mathrm{R}^3$ is the measured marker positions, $\boldsymbol{p}_i(\boldsymbol{q}) \in \mathrm{R}^3$ is marker positions calculated by $\boldsymbol{q}$, $l_j(\boldsymbol{q})$ is the wire length for tendons, ligaments and cartilages, $\hat{l}_j$ is natural length of wires, N_T is total number of wires. The original kinetic data from the instrumented wheels were re-calculated with respect to a point from the subject's palm selected as an origin by using the force-moment balance equation.

$$\boldsymbol{F_h} = \begin{bmatrix} \boldsymbol{I} & \boldsymbol{0} \\ \boldsymbol{P}\times\boldsymbol{I} & \boldsymbol{I} \end{bmatrix}^{-1} \boldsymbol{F_s} \tag{6}$$

where, $\boldsymbol{F_h} \in \mathrm{R}^6$ is the vector of the forces and moments applied by subject's palm, $\boldsymbol{F_s} \in \mathrm{R}^6$ is the vector of the measured forces and moments in the global coordinate system, $\boldsymbol{P} \in \mathrm{R}^3$ is the position vector from the origin of the six-axis force sensor to the subject's palm, $\boldsymbol{I} \in \mathrm{R}^3$ is an unit vector. Then, the standard Newton–Euler inverse dynamics algorithm [26] was applied to the given motion data of $\boldsymbol{q}, \dot{\boldsymbol{q}}, \ddot{\boldsymbol{q}}$ and $\boldsymbol{F_h}$ for calculation of the intersegmental joint forces $\boldsymbol{F_H}(\boldsymbol{q}, \dot{\boldsymbol{q}}, \ddot{\boldsymbol{q}}, \boldsymbol{F_h})$ and torques $\boldsymbol{\tau_H}(\boldsymbol{q}, \dot{\boldsymbol{q}}, \ddot{\boldsymbol{q}}, \boldsymbol{F_h})$.

This way, the muscle forces were calculated with respect to the joint torques. Since the number of the muscles that drive the joints is greater than the degrees of freedom of the arm, the case belongs to the class of ill-posed problems. The distribution of the muscle forces was calculated by using the following optimization algorithm:Find $\boldsymbol{f}$ that minimizes

$$Z = \frac{w_1}{2}\left|\boldsymbol{\tau_H}(\boldsymbol{q}, \dot{\boldsymbol{q}}, \ddot{\boldsymbol{q}}, \boldsymbol{F_h}) - \boldsymbol{K}(\boldsymbol{q})\boldsymbol{f}\right|^2 + \frac{w_2}{2}\left|\boldsymbol{f}\right|^2 \tag{7}$$

subject to

$$\boldsymbol{f} \leq \boldsymbol{0} \tag{8}$$

where, $\boldsymbol{f} \in \mathrm{R}^{N_W}$ is a force vector for muscle, tendons, ligaments and cartilages, N_W is total number of muscle, tendons, ligaments and cartilages, $\boldsymbol{K}(\boldsymbol{q}) \in \mathrm{R}^{N_J \times N_W}$ is a projection matrix from $\boldsymbol{f}$ to joint torques, w_1 and w_2 are weighting parameters. Shoulder joint contact force, which indicates the joint surface loading, is computed as a synthetic vector of the intersegmental force for shoulder joint acquired from the inverse dynamics analysis and the compressive forces from muscles, tendons, ligaments and cartilages crossing the shoulder joint.

Statistics

Statistical analyses were performed by using the Tukey–Kramer method [27]. All data were expressed as mean ± standard deviation (SD). The level of significance was set at $P < 0.05$.

Results

Kinematic and kinetic data

Conducted experiments showed that the cadence (the number of propulsion strokes per a unit time) has its lowest value during the lever propulsion test with a gear ratio 1.5. The cadence increased when the gear ratio of the lever propulsion tests was lowered (Fig. 6). The cadence during the handrim propulsion test for road inclination angles of 2° or 4° had quite similar values to the cadence during the lever propulsion test with a gear ratio of 1.

The time from the wheelchair propulsion cycle during which propulsion torque is applied to the rear wheel axis, was defined as a push phase. For easer comparison of the results, the push phases were presented as percentage from the whole propulsion cycle. Results revealed that the percentage of the push phase during the handrim propulsion experiment was noticeably higher than the lever propulsion push phase (Fig. 7). The percentage of the push phase for both propulsion systems tended to increase as the road inclination angle increased. The percentage of the push phase dropped significantly when the lever propulsion gear ratio was decreased from 1.5 to 1/1.5.

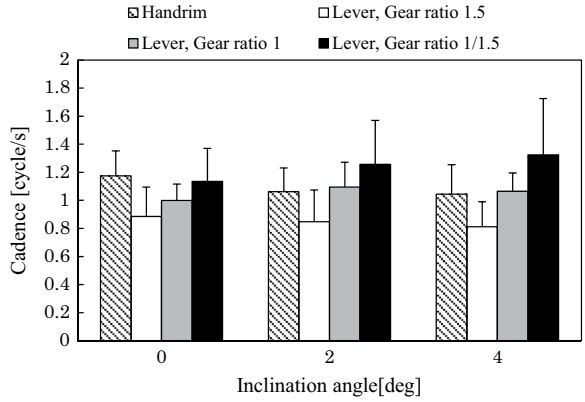

Fig. 6 Cadence for different road inclination angles

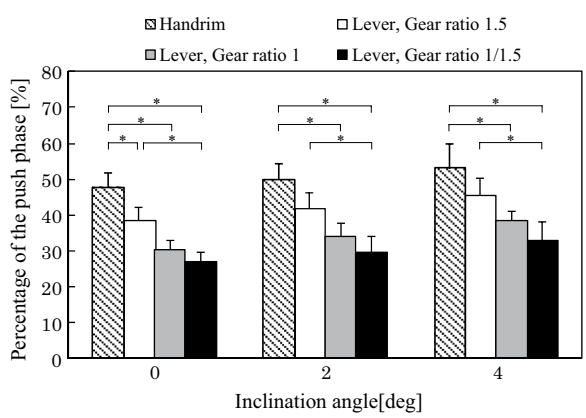

Fig. 7 Percentage of the push phase in one driving period (* $P < 0.05$)

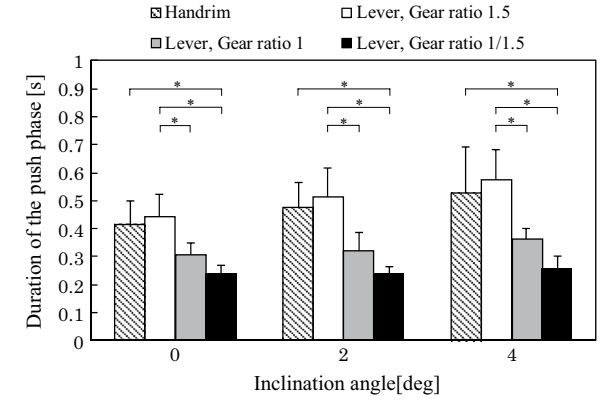

Fig. 8 Duration of the push phase (* $P < 0.05$)

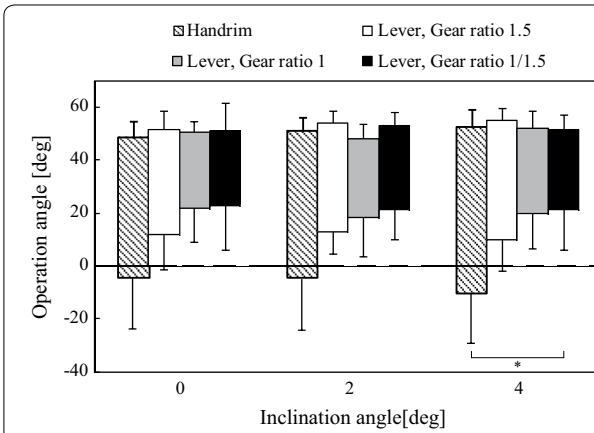

Fig. 9 Operation angle of the handrim and lever (* $P < 0.05$)

The push phase of the handrim propulsion test was longer than the push phase of the lever propulsion with a gear ratio of 1 for all inclination angles but shorter than the push phase of the lever propulsion with gear ratio of 1.5 (Fig. 8). The propulsion time shortened significantly when the gear ratio of the lever propulsion was reduced from 1.5 to 1/1.5.

The push angle for the handrim propulsion was defined as the difference between the start angle (the angle around the handrim center determined by the point where hand establishes initial contact with the handrim) and the end angle (the angle at the point where the hand releases from the handrim of wheelchair). The push angle for the lever propulsion was defined as the difference between the start angle (the angle at the point where the user starts to apply force to the lever) and the position where the forward pushing of the lever ends. The push angle in this case is measured with regard to the lever's centre of rotation. The push angles θ_p for handrim propulsion and lever propulsion are indicated in Figs. 3 and 9 respectively. Results showed that the start angle during the lever propulsion tasks shifted forward when the gear ratio got smaller, and remained constant when the gear ratio was set to 1. The end angle of the lever push phase remained almost the same for all driving tests. It was revealed that the handrim push angle was larger than the lever propulsion push angle. Results also showed that the lever propulsion push angle became smaller when the gear ratio was reduced.

The amplitude of the input torque imposed by the subject to the wheelchair increased when the road inclination angle was increased in both drive systems (Fig. 10). The generated input torque during the lever propulsion experiment decreased when the gear ratio became smaller, but it always remained greater than the torque imposed by the subject during the handrim propulsion.

Figure 11 presents the maximum propulsion torque transferred to the rear wheels for each road inclination. It can be observed that the user had to generate a higher

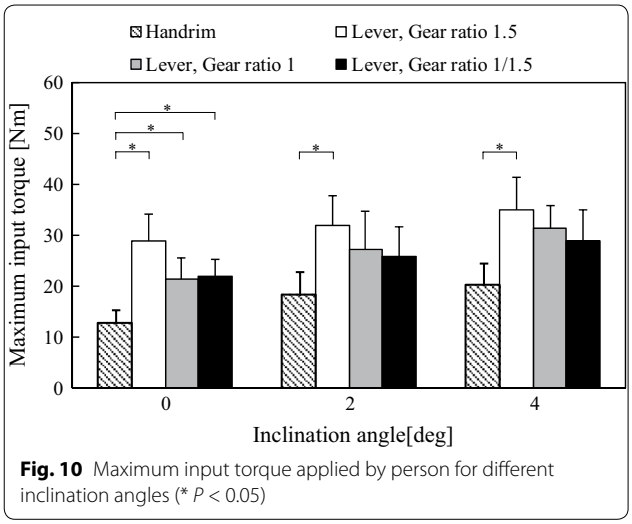

Fig. 10 Maximum input torque applied by person for different inclination angles (* $P < 0.05$)

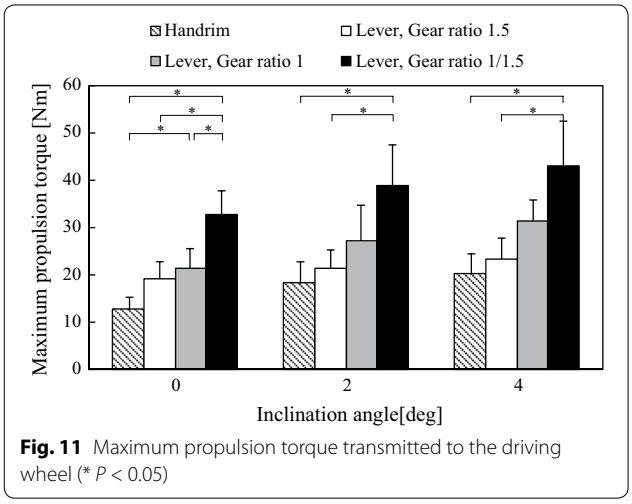

Fig. 11 Maximum propulsion torque transmitted to the driving wheel (* $P < 0.05$)

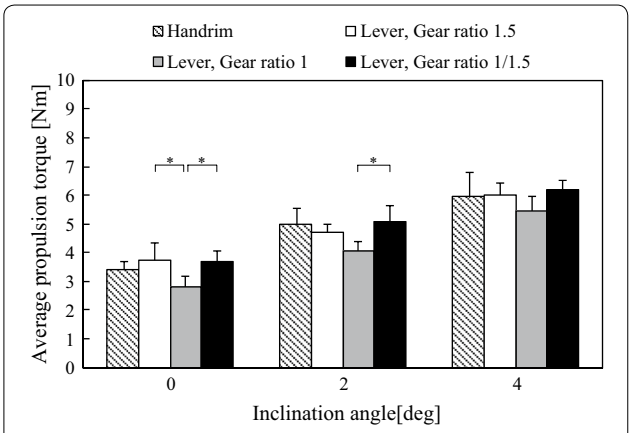

Fig. 12 Average propulsion torque in 1 propulsion cycle (* $P < 0.05$)

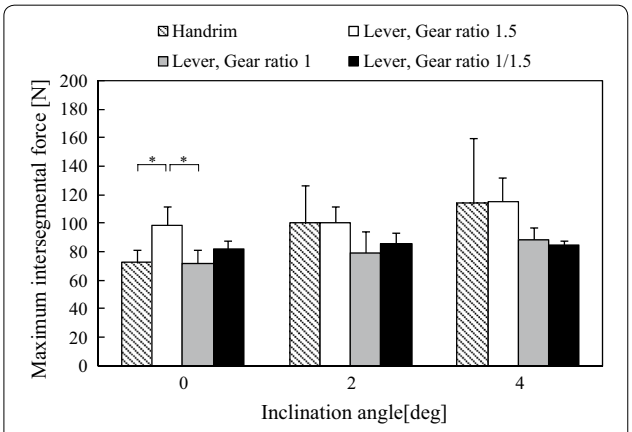

Fig. 13 Maximum shoulder intersegmental force (* $P < 0.05$)

torque when the road inclination increased in order to maintain the target wheelchair speed. The maximum torque during the lever propulsion tests dropped when the gear ratio was increased, but remained greater than the propulsion torque in the handrim propulsion experiment. It was found that the average propulsion torques for lever propulsion and handrim propulsion had quite similar values for the same road inclination (Fig. 12).

Biodynamic data

Figure 13 and Table 1 present the maximum intersegmental force of the shoulder joint computed by inverse dynamics analysis. Results show that during lever propulsion with a gear ratio of 1.5 the intersegmental forces are greater than the intersegmental forces for lever propulsion with gear ratios 1 and 1/1.5. For road inclination of 2 and 4 degrees, the intersegmental force during the lever propulsion with a gear ratio of 1.5 was almost comparable to that of the handrim propulsion.

Figure 14 and Table 1 show the maximum shoulder joint contact force for the lever propulsion and handrim propulsion experiments. Results revealed that the

Table 1 The ratio of shoulder load during lever propulsion to the shoulder load during handrim propulsion

Shoulder joint	Inclination angle (°)	Handrim	Gear ratio of Lever propulsion mechanism		
			1.5	1	1/1.5
Intersegmental force	0	1.0 (72 N)	1.4	1.0	1.1
	2	1.0 (100 N)	1.0	0.8	0.9
	4	1.0 (114 N)	1.0	0.8	0.7
Contact force	0	1.0 (863 N)	0.9	0.6	0.7
	2	1.0 (1519 N)	0.6	0.4	0.4
	4	1.0 (1827 N)	0.6	0.4	0.3

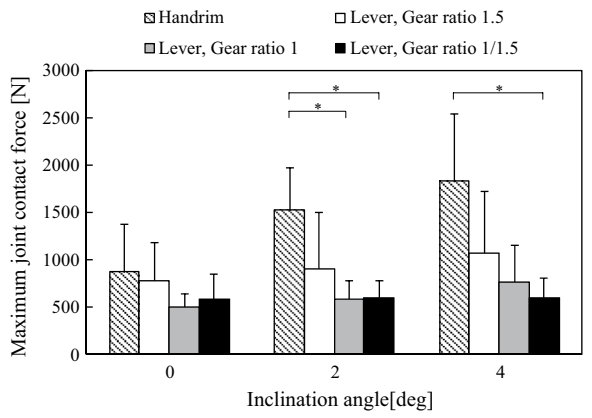

Fig. 14 Maximum shoulder joint contact force (* $P < 0.05$)

shoulder joint contact force during the handrim propulsion is significantly greater compared to shoulder joint contact forces during the all lever propulsion tests. The difference became bigger when the terrain inclination was increased. The shoulder joint contact force declined when the lever propulsion gear ratio was decreased from 1.5 to 1/1.5.

Discussion

Validity of the musculoskeletal model

We compared our results for the shoulder joint contact force during handrim propulsion with the results reported previously by other researchers. The maximum contact force of the shoulder joint estimated with our approach was 863 N (average 542 N) for the test that simulated wheelchair motion on a flat surface, 1519 N (average 780 N) for motion on a ramp inclined on 2 degrees (equivalent to about 8 W) and 1827 N (average 907 N) in the test simulating wheelchair motion on a ramp with a gradient angle of 4° (about 16 W). Van der Helm et al. reported that the average contact force of the shoulder joint during handrim propulsion reached 1900 N when the load to the driving wheels was set to 40 % of the maximal torque that the individual is able to apply to the same wheel [17]. Veeger et al. conducted a propulsion experiment where the target speed was set to 3 km/h. Their results revealed that the maximum shoulder joint contact force was about 780 N (average 510 N) for a road resistance of 10 W and about 1070 N (average 720 N) for equivalent road resistance of 20 W [18]. Melissa et al. conducted handrim propulsion experiments where the subjects propelled a wheelchair on a self-selected speed. Maximum shoulder joint contact force was 702 N (average 250 N) on a flat surface and 2555 N (average 830 N) for propulsion on a ramp with 1:12 incline (an inclination angle of 4.8°) [19]. As explained above, our approach was based on the nMotion musculous musculoskeletal model. The comparison of our results with the results reported in the other studies showed that our shoulder joint contact force results are quite similar to the results obtained by the other researchers.

Bergmann et al. conducted in vivo measurement of shoulder joint contact force. They showed that the shoulder joint contact force reached 1700 N (238 % of body weight) during forward flexion more than 90 degrees with 2 kg weight in the hand [28]. They also showed a reasonable compatibility between the shoulder joint contact force estimated by a musculoskeletal model and the measured force [29]. However, it was also discovered that the results based on the musculoskeletal model depend on the direction of force application and user's posture. These findings suggest that computational procedures for estimating muscle force and shoulder joint contact force should be improved in future studies. However, within the scope of the present study, the musculoskeletal model analysis can be used successfully for estimation of shoulder joint contact force and simple comparison of the parameters of wheelchair propulsion systems.

Lever propulsion on a gear ratio 1.5

It was observed that the average propulsion torque during handrim propulsion and the lever propulsion on a gear ratio of 1.5 had quite similar values (Fig. 12). The reason for that result could be the selected dimensions of the handrim and the lever.In this experiment we used a handrim with a radius of 266.7 mm and a lever which length was 420 mm, which gives a ratio between the moment arms 1:1.57 (420/266.7). Sequentially, the virtual moment arm for the lever propulsion with gear ratio 1.5 was 1.05 (the ratio of the moment arm/gear ratio = 1.57/1.5), which is almost the same as the virtual moment arm for the lever propulsion. Considering that, the similarity of the average propulsion torques during the handrim propulsion and lever propulsion on a gear ratio of 1.5 can be explained with the similarity of the virtual moment arms (1:1.05). Although the average propulsion torques during the handrim propulsion and the lever propulsion of a gear ratio of 1.5 were almost the same, it was observed that the cadence and the shoulder joint contact force during the handrim propulsion were greater (Figs. 6, 14; Table 1). This result suggests that during the handrim propulsion the target speed can be maintained by increase of the cadence and high load is applied repeatedly to the joints. This result also shows that lever propulsion on a gear ratio of 1.5 can reduce shoulder joint contact force up to 40 % compared to handrim propulsion. As presented in Fig. 13, maximum intersegmental forces during handrim propulsion and lever propulsion at gear ratio 1.5 are comparable for road

inclination angles of 2° and 4°, which indicates that the musculoskeletal model that we used for estimation of the shoulder joint contact force considers precisely the muscle forces and can be used for comparison of joint loads.

Lever propulsion on a gear ratio of 1

It was observed that for inclination angles of 2° and 4°, the cadence during the lever propulsion on a gear ratio of 1 was almost the same as the cadence of handrim propulsion (Fig. 6). However, the push phase of the lever propulsion was shorter (Fig. 8). It was also observed that lever propulsion on a gear ratio of 1 reduced shoulder joint contact force up to 60 % compared to handrim propulsion.

Lever propulsion on a gear ratio of 1/1.5

Figure 12 shows that the average propulsion torque during handrim propulsion and the torque during lever propulsion on a gear ratio 1/1.5 were similar. However, the lever propulsion with gear ratio 1/1.5 is equivalent to much longer virtual moment arm. For the selected handrim diameter and lever length, the ratio between the moment arms of the handrim and the lever is 1:2.36. Because of the longer virtual moment arm, the required propulsion torque is achieving with much lower push force, which reduces shoulder joint force. This result shows that lever propulsion on a gear ratio of 1/1.5 can reduce shoulder joint contact force up to 70 % compared to handrim propulsion (Fig. 14; Table 1). The results also show that the push phase during the lever propulsion was significantly shorter (Fig. 8) than the push phase during the handrim experiment which suggests that the cadence has been increased for sustaining the target speed (Fig. 6). Further shortening of the push phase was observed when the gear ratio of the lever propulsion was reduced from 1.5 to 1/1.5. Respectively, the cadence increased additionally to sustain the wheelchair speed.

Conclusions

We conducted series of experiments and obtained quantitative results about the shoulder joint contact force for lever propulsion on three different gear ratios of the lever propulsion mechanism. These results were also compared with the experimental results from a handrim propulsion test. For our trials we developed a special mechatronic wheelchair simulator that allowed simulation of different gear ratios of the lever propulsion mechanism. Further, we examined the effect of the gear ratio of lever-propulsion mechanism on the shoulder joint contact force. For that purpose, we also conducted series of experiments where the gear ratio was varied from 1.5 to 1 and 1/1.5. Experimental results showed that shoulder joint contact force during lever propulsion mechanism with gear ratio 1/1.5 was up to 70 % lower than the shoulder joint contact force during handrim propulsion. Although this study was limited to three gear ratios of the propulsion mechanism, it evidences the positive effect of the lever propulsion mechanisms with gear ratio. Our plan is to conduct further lever-propulsion experiments for different gear ratios and target speeds. In the future, we also intend to expand the initial results obtained within this study by making new tests with a bigger number of participants, including wheelchair users.

Authors' contributions

MS contributed to the conception, design of experiments, acquisition of data, analysis and interpretation of data and drafting of the manuscript. DS took part in the conception, interpretation and revising of the manuscript. YO took part in the experiments and calculations. HM and AN took part in the calculations of the experimental data by using the musculoskeletal model. All authors read and approved the final manuscript.

Author details

[1] Graduate School of Engineering, Iwate University, Morioka, Iwate, Japan. [2] School of Science and Technology, Middlesex University, London, UK. [3] Department of Intelligent Systems Engineering, Ichinoseki National College of Technology, Ichinoseki, Iwate, Japan.

Acknowledgements

This study was supported in part by the Program for Revitalization Promotion (H24MoriII-217), Japan Science and Technology Agency.

Compliance with ethical guidelines

Competing interests

The authors declare that they have no competing interests.

Received: 8 March 2015 Accepted: 25 September 2015
Published online: 03 October 2015

References

1. Brubaker CE, McClay IS, McLaurin C (1984) Effect of seat position on wheelchair propulsion efficiency. In: Proc. the 2nd International Conference on Rehabilitation Engineering, pp 12–14
2. van der Woude LH, Hendrich KM, Veeger HE, van Ingen Schenau GJ, Rozendal RH, de Groot G, Hollander AP (1988) Manual wheelchair propulsion: effects of power output on physiology and technique. Med Sci Sports Exerc 20(1):70–78
3. Hintzy F, Tordi N (2004) Mechanical efficiency during hand-rim wheelchair propulsion: effects of base-line subtraction and power output. Clin Biomech 19(4):343–349
4. van der Woude LH, Veeger HE, Dallmeijer AJ, Janssen TW, Rozendaal LA (2001) Biomechanics and physiology in active manual wheelchair propulsion. Med Eng Phys 23(10):713–733
5. de Groot S, Veeger HE, Hollander AP, van der Woude LH (2002) Consequence of feedback-based learning of an effective hand rim wheelchair force production on mechanical efficiency. Clin Biomech 17(3):219–226
6. Sasaki M, Iwami T, Miyawaki K, Sato I, Obinata G, Dutta A (2010) Higher dimensional spatial expression of upper limb manipulation ability based on human joint torque characteristics. In: Lazinica A, Kawai H (ed) Robot manipulators, new achievements. INTECH
7. Curtis KA, Dillon DA (1985) Survey of wheelchair athletic injuries: common patterns and prevention. Paraplegia 23:170–175
8. Gellman H, Chandler DR, Petrasek J, Sie I, Adkins R, Waters RL (1988) Carpal tunnel syndrome in paraplegic patients. J Bone Joint Surg 70(4):517–519
9. Sie IH, Waters RL, Adkins RH, Gellman H (1992) Upper extremity pain in postrehabilitation spinal cord injured patient. Arch Phys Med Rehabil 73:44–48

10. Pentland WE, Twomey LT (1994) Upper limb function in persons with long-term paraplegia and implications for independence: part I. Paraplegia 32:211–218
11. Hughes CJ, Weimar WH, Sheth PN, Brubaker CE (1992) Biomechanics of wheelchair propulsion as a function of seat position and user-to-chair interface. Arch Phys Med Rehabil 73(3):263–269
12. Cooper RA (1998) Wheelchair selection and configuration. Demos Medical Publishing, New York
13. Sasaki M, Kimura T, Matsuo K, Obinata G, Iwami T, Miyawaki K, Kiguchi K (2008) Simulator for optimal wheelchair design. J Robot Mechatron 20(6):854–862
14. Sasaki M, Ota Y, Hase K, Stefanov D, Yamaguchi M (2014) Simulation model of a lever-propelled wheelchair, In: Proc. the 36th Annual International Conference of the IEEE Engineering in Medicine and Biology Society, pp 6923–6926
15. Requejo PS, Lee SE, Mulroy SJ, Haubert LL, Bontrager EL, Gronley JK, Perry J (2008) Shoulder muscular demand during lever-activated vs pushrim wheelchair propulsion in persons with spinal cord injury. J Spinal Cord Med 31(5):568–577
16. Lui J, MacGillivray MK, Sheel AW, Jeyasurya J, Sadeghi M, Sawatzky BJ (2013) Mechanical efficiency of two commercial lever-propulsion mechanisms for manual wheelchair locomotion. J Rehabil Res Dev 50(10):1363–1372
17. van der Helm FC, Veeger HE (1996) Quasi-static analysis of muscle forces in the shoulder mechanism during wheelchair propulsion. J Biomech 29(1):39–52
18. Veeger HE, Rozendaal LA, van der Helm FC (2002) Load on the shoulder in low intensity wheelchair propulsion. Clin Biomech 17(3):211–218
19. Morrow MM, Kaufman KR, An KN (2010) Shoulder model validation and joint contact forces during wheelchair activities. J Biomech 43(13):2487–2492
20. Nakamura Y, Yamane K, Fujita Y, Suzuki I (2005) Somatosensory computation for man-machine interface from motion-capture data and musculoskeletal human model. IEEE Trans Robot 21(1):58–66
21. Yamane K, Fujita Y, Nakamura Y (2005) Estimation of physically and physiologically valid somatosensory information, In: Proc. the 2005 IEEE International Conference on Robotics and Automation, pp 2635–2641
22. Higashihara A, Nagano Y, Ono T, Fukubayashi T (2014) Relationship between the peak time of hamstring stretch and activation during sprinting. Eur J Sport Sci 31:1–6
23. Kita T, Yamamoto M, Maeda A (2014) Relationship between lower extremity motions and release time of baseball infielders while fielding grounders. Int J Sport Health Sci 12:17–23
24. Kageyama M, Sugiyama T, Takai Y, Kanehisa H, Maeda A (2014) Kinematic and kinetic profiles of trunk and lower limbs during baseball pitching in collegiate pitchers. J Sport Sci Med 13:742–750
25. Nagano Y, Higashihara A, Takahashi K, Fukubayashi T (2014) Mechanics of the muscles crossing the hip joint during sprint running. J Sports Sci 32(18):1722–1728
26. Orin D, McGhee R, Vukobratovic M, Hartoch G (1979) Kinematic and kinetic analysis of open-chain linkages utilizing Newton-Euler method. Math Biosci 43:107–130
27. Kramer CY (1956) Extension of multiple range tests to group means with unequal numbers of replications. Biometrics 12:307–310
28. Bergmann G, Graichen F, Bender A, Rohlmann A, Halder A, Beier A, Westerhoff P (2011) In vivo gleno-humeral joint loads during forward flexion and abduction. J Biomech 44(8):1543–1552
29. Nikooyan AA, Veeger HE, Westerhoff P, Graichen F, Bergmann G, van der Helm FC (2010) Validation of the delft shoulder and elbow model using in vivo glenohumeral joint contact forces. J Biomech 43(15):3007–3014